J. Fluid Mech. (1972), *vol.* 56, *part* 2, *pp.* 201–219
Printed in Great Britain

A free-streamline theory for bluff bodies attached to a plane wall

By MASARU KIYA AND MIKIO ARIE
Faculty of Engineering, Hokkaido University, Sapporo, Japan

(Received 22 June 1972)

A free-streamline theory is presented for the separated flow past two-dimensional bluff bodies attached to a long plane wall on which a turbulent boundary layer has developed. The non-uniform velocity profile in the turbulent boundary layer which would be measured if the bluff bodies were absent has been replaced by a hypothetical inviscid parallel shear flow which has a constant vorticity. This model admits analytical solutions and automatically yields closed streamlines in front of the bluff bodies such as the normal plate and the semicircular projection, which are geometrically very similar to observed front separation bubbles. The present theory involves three or four parameters which must be determined on the basis of experimental information, the number of parameters depending upon the shape of bluff bodies. Two typical examples of bluff bodies, i.e. the normal plate and the semicircular projection, are worked out. Pressure distributions around these bodies predicted by the present theory are found to give a good agreement with experimental measurements.

1. Introduction

The main feature of flow past a bluff body is its separation from the body surface, well ahead of the rear stagnation point, and the formation of a broad wake. The separated boundary layer continues downstream as a free shear layer, which is well defined at first and forms a boundary between the wake and the distorted inviscid outer flow. Because of the complex nature of the wake dynamics, including the formation of organized vortex systems and the lack of knowledge of the link between wake and separation conditions, realistic theoretical models of the separated flow past a bluff body have included some empiricism.

From a practical point of view, one of the most valuable results of any theoretical analysis of the separated flows at high Reynolds number is the prediction of the pressure distribution around a bluff body. A theoretical analysis of the time-averaged separated flow past a bluff body in a uniform flow was initiated by Helmholtz and Kirchhoff. They considered the two-dimensional incompressible flow past flat plates behind which extended constant-pressure wakes of infinite extent, by means of the conformal transformations. These constant-pressure wakes whose boundaries are so-called free streamlines grow infinitely wide with increasing downstream distance, and thus are improper representations of the actual wakes. Another defect of the constant-pressure wake model comes

from the basic assumption that the pressure everywhere in the wake is equal to the pressure outside the wake at infinity, or, in other words, that the pressure coefficient defined by $C_{pb} = (p_b - p_\infty)/\frac{1}{2}\rho U_\infty^2$, where p_∞ and p_b are the pressures at infinity outside the wake and at any point within the wake, ρ is the density of fluid and U_∞ is the mainstream velocity, must vanish. In actual wakes, however, the base pressure p_b is observed to be much lower than p_∞, and thus C_{pb} is always negative. The base pressure is low enough to produce significant discrepancies between the results obtained from the Helmholtz–Kirchhoff model and experiment. For example, the drag coefficient measured for a flat plate is 1·95, whereas the Helmholtz–Kirchhoff model yields 0·88.

Some modifications of the Helmholtz–Kirchhoff model were made to allow arbitrary base pressures by Roshko (1955), Wu (1962, who refined the theory of Roshko), Woods (1955) and Parkinson & Jandali (1970). Woods' theory, in particular, can be applied to compressible subsonic flow about given curved bodies. These theories have given pressure distributions around bluff bodies in good agreement with experimental measurements in the case of Reynolds numbers, which will hereafter be denoted by *Re*, of order greater than 10^3.

However, when applied to the case of lower Reynolds number, in which separated flows are rather steady, these models are generally unsatisfactory, even when, as in Roshko's (1955) case, the wake pressure is set equal to that measured experimentally along the non-wetted surface of the body. This fact was pointed out by Acrivos *et al.* (1965) for the pressure distribution around a circular cylinder, the Reynolds number being of order 10^2. Thus they developed a new method which consisted simply of an inviscid analysis around a suitable composite body (circular arc plus assumed wake boundary) together with the assumption of zero pressure drop in the vertical direction through the wake. The calculated pressure profiles on the cylinder surface for $Re = 40$, 129 and 177 not only agreed with the experimental measurements but were relatively insensitive to the shape of the assumed body contour.

All the theories discussed above are concerned with two-dimensional bluff bodies located in a uniform stream of infinite extent. In practice, however, there are many examples of bluff bodies which are attached to a plane wall† on which a turbulent boundary layer develops, typical examples being roughness elements or part of an orifice or a valve. Buildings are also examples of this category of much larger scale. Upstream of a bluff body, an adverse pressure gradient will be produced by the deflexion of the flow by the bluff body. The boundary layer will be forced to separate from the plane wall and will reattach on the front surface of the bluff body, thereby enclosing a front separation bubble. In the cases of the normal plate, the rectangular cylinder and the semicircular projection, flow visualization techniques have shown that the mean flow inside and outside the front separation bubble is quite steady. The streamline which separates from the plane wall, and divides the main flow from the separated flow, must therefore be the streamline which reattaches to the bluff body. Observations for the case of a normal plate also show that the length of the front separation bubble is of the

† In this paper the wall to which bluff bodies are attached will be referred to as the 'plane wall'.

same order as the plate height, and about 60 % of the upstream face of the normal plate is exposed to the separated flow.

The effects of the front separation bubble are manifested in the pressure distributions around the front part of a bluff body. Good & Joubert (1968) have shown experimentally that, when normalized by maximum pressure, the pressure distributions on the normal plates exhibit approximately similar profiles which have a maximum at about $y'/h = 0{\cdot}6$, where y' is the distance along the flat plate measured from the plane wall (this may be clearly seen in figure 15 of Good & Joubert 1968). Also the pressure distributions on the plane wall upstream the normal plate are roughly constant in the region exposed to the front separation bubbles (Good & Joubert 1968, figure 4). Analogous pressure distributions have been observed for rectangular cylinders (Arie *et al.* 1972) and semicircular projections (Sakamoto & Moriya 1973).

A theory describing the separated flow past a bluff body attached to the plane wall must therefore include the front separation bubble, together with the non-uniformity of the undisturbed velocity profile in the boundary layer. The effects of non-uniform velocity profiles will become theoretically tractable if an inviscid shear flow can be employed as a suitable model. Since, of all inviscid shear flows, the uniform shear flow which has a constant vorticity is easiest to treat analytically, it will be useful to examine the applicability of this model. In this connexion it should be noted that Fraenkel (1961) has obtained local solutions for the inviscid uniform shear flow past an acute corner (of included angle less than or equal to $\frac{1}{2}\pi$ measured on the side of the fluid) on an otherwise arbitrary boundary to show that a corner eddy is formed under certain circumstances. The flow pattern around a semicircular projection, which was worked out by Fraenkel, includes closed streamlines akin to the experimentally observed separation bubble in front of the semicircular projection. The same kind of closed streamlines had been obtained by Yih (1959) for the inviscid shear flow of cosine velocity profile in a two-dimensional channel. Although the mechanisms of flow in these closed streamlines may not be exactly the same as those in the actual front separation bubbles, a striking geometrical similarity between these two flow patterns justifies choosing the uniform shear flow as a model of the turbulent boundary layer developing on the plane wall to which bluff bodies are attached.

Upon the basis of this model, this paper gives a free-streamline theory for the separated flows past bluff bodies attached to a plane wall, together with a comparison of the theory with some experimental measurements.

2. General theory

We consider the two-dimensional, incompressible, inviscid, steady flow past a bluff body (ASC) with separation at the point S, which is attached to a plane wall represented by the real axis of the z plane, as shown in figure 1. Throughout this paper, Cartesian co-ordinates are non-dimensionalized by a representative length l and the corresponding velocity components are non-dimensionalized by

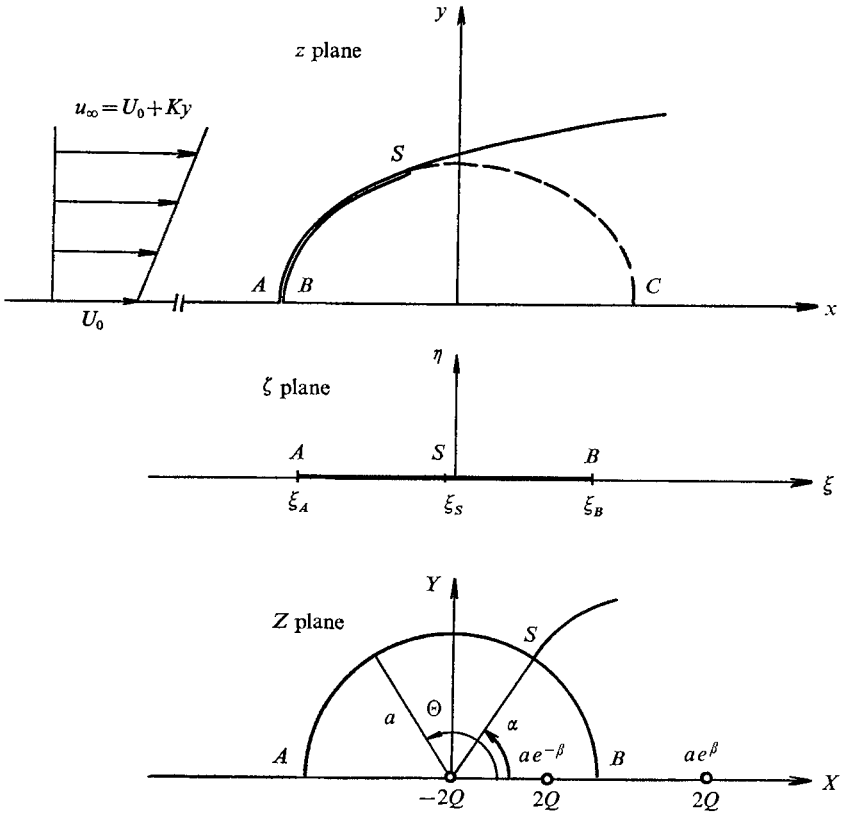

FIGURE 1. Physical plane and transform planes.

a representative velocity U_{ref}. The velocity profile at infinitely large distances from the body is described by a uniform shear flow

$$u_\infty = U_0 + Ky, \quad v_\infty = 0,$$

where U_0 is the non-dimensional speed at infinity on the x axis and K is the velocity gradient non-dimensionalized by U_{ref}/l.

Now we replace the wetted surface AS of the body contour ASC by the slit ASB. The remaining part SC of the body contour lies in the wake region and is therefore ignored in the present analysis. For the sake of brevity, the boundary of the fluid domain $\mathscr{F}$, which consists of the x axis and the slit, is designated as $\mathscr{B}$. It is well established in the theory of conformal transformations that the domain $\mathscr{F}$ can be mapped conformally onto an upper half-plane. Let

$$z = f(\zeta), \tag{2.1}$$

where $z = x + iy$ and $\zeta = \xi + i\eta$, be one of these transformations, such that the points A and B in the z plane map onto $\xi = \xi_A$ and $\xi = \xi_B (\xi_A < \xi_B)$, respectively, in the ζ plane. The boundary $\mathscr{B}$ naturally maps onto the ξ axis of the ζ plane.

A stream function ψ is introduced by the definition

$$\partial\psi/\partial y = u, \quad \partial\psi/\partial x = -v,$$

where ψ is non-dimensionalized by $U_{\text{ref}} l$. Thereby the equation of continuity is automatically satisfied and Euler's equations of motion for steady flow are simply reduced to

$$\Delta\psi = K, \tag{2.2}$$

where

$$\Delta = \partial^2/\partial x^2 + \partial^2/\partial y^2.$$

The boundary conditions for ψ are

$$\left.\begin{aligned} \psi &= \text{constant} \quad \text{on} \quad \mathscr{B}, \\ \partial\psi/\partial x \to 0, \quad \partial\psi/\partial y &\to U_0 + Ky \quad \text{as} \quad |z| \to \infty \text{ in } \mathscr{F}. \end{aligned}\right\} \tag{2.3}$$

If ψ is subdivided into two parts, i.e.

$$\psi = \tfrac{1}{2}Ky^2 + \Psi,$$

Ψ satisfies the Laplace equation

$$\Delta\Psi = 0. \tag{2.4}$$

Accordingly, by the introduction of a function Φ which is related to Ψ by the Cauchy–Riemann equations

$$\partial\Phi/\partial x = \partial\Psi/\partial y, \quad \partial\Phi/\partial y = -\partial\Psi/\partial x,$$

the complex function defined by $W = \Phi + i\Psi$ becomes an analytic function of z. At the same time the boundary conditions (2.3) are transformed to

$$\left.\begin{aligned} \Psi + \tfrac{1}{2}Ky^2 &= \text{constant} \quad \text{on } \mathscr{B}, \\ \partial\Psi/\partial x \to 0, \quad \partial\Psi/\partial y &\to U_0 \quad \text{as} \quad |z| \to \infty \quad \text{in } \mathscr{F}. \end{aligned}\right\} \tag{2.5}$$

Assuming that (2.1) behaves as

$$z \sim k_1\zeta + k_2 \ln\zeta + k_3 + O(\zeta^{-1}) \quad (k_1, k_2 \text{ real}) \tag{2.6}$$

for $|\zeta| \to \infty$, Fraenkel (1961) has obtained the solution of (2.4) which satisfies the boundary conditions (2.5), i.e.

$$\Psi = \mathscr{I}(W_u + W_s), \tag{2.7}$$

where $\mathscr{I}$ means 'the imaginary part of' and

$$W_u = \Phi_u + i\Psi_u = U_0 k_1 \zeta \tag{2.8}$$

and

$$W_s = \Phi_s + i\Psi_s = \frac{K}{2\pi}\int_{\xi_A}^{\xi_B} \frac{y^2(\xi^*, 0)}{\zeta - \xi^*}\, d\xi^*. \tag{2.9}$$

In order to have a free streamline which originates from the separation point S and extends in the downstream direction we add to (2.7) the flow from a combination of sinks and sources which are properly located in the z plane. This approach has been adopted by Parkinson & Jandali (1970) in a theory for two-dimensional separated flow of an incompressible fluid past a symmetrical bluff body in a uniform stream of infinite extent. For this purpose a third complex plane Z is introduced by the definition

$$\zeta = Z + (a^2/Z) + \tfrac{1}{2}(\xi_A + \xi_B), \tag{2.10}$$

where $Z = X + iY$ and $a = \frac{1}{2}(\xi_B - \xi_A)$. The transformation (2.10) maps the slit ASB in the z plane onto a semicircular projection ASB of radius a with centre at the origin of the Z plane. In the Z plane the combination of a source pair of strength $2Q$ located at $(ae^{\pm\beta}, 0)$, where β is real or purely imaginary, and its image sink of strength $2Q$ at the origin satisfies the boundary condition on the semicircular projection and, by symmetry, the X axis can be considered as a solid boundary. The complex potential W_Q of the source–sink system is given by

$$W_Q = (Q/\pi)\{\ln(Z - ae^{\beta}) + \ln(Z - ae^{-\beta}) - \ln Z\}. \tag{2.11}$$

If β is real, source pairs are located on the X axis, while if β is purely imaginary, say $\beta = i\delta$, source pairs are symmetrically located at angles $\pm\delta$ on the circle which is formed by the semicircular projection ASB and its reflexion on the lower half of the Z plane. The implications of β being real or purely imaginary will be discussed later in § 3.

When W_Q is added to (2.7) the stream function ψ of the resulting flow is

$$\psi = \tfrac{1}{2}Ky^2 + \mathscr{I}(W_u + W_s + W_Q) \tag{2.12}$$

and the complex velocity in the z plane becomes

$$\begin{aligned} u - iv &= Ky + \frac{dW_u}{dz} + \frac{dW_s}{dz} + \frac{dW_Q}{dz} \\ &= Ky + \left(\frac{dW_u}{d\zeta} + \frac{dW_s}{d\zeta} + \frac{dW_Q}{dZ}\frac{dZ}{d\zeta}\right)\Big/\frac{dz}{d\zeta}. \end{aligned} \tag{2.13}$$

Since the angle of intersection of curves at S is doubled in the z plane, the point S is a critical point of the transformation (2.1), where $dz/d\zeta = f'(\zeta)$ has a simple zero. Therefore, in order that the velocity at the point S is finite, we must have

$$\left(\frac{dW_u}{d\zeta} + \frac{dW_s}{d\zeta} + \frac{dW_Q}{dZ}\frac{dZ}{d\zeta}\right)_{\zeta=\zeta_s} = 0, \tag{2.14}$$

where ζ_s denotes the location of S in the ζ plane. Equation (2.14) determines Q in terms of U_0, K and β. Because of the doubling of the angle at S, the stagnation streamline leaving S in the Z plane becomes the tangential separation streamline at S in the z plane.

Since the non-dimensional vorticity $-\Delta\psi$, which equals $-K$, is constant throughout the flow field, Bernoulli's equation can be written in the form

$$p_\infty + \tfrac{1}{2}(u_\infty^2 + v_\infty^2) - K\psi_\infty = p + \tfrac{1}{2}(u^2 + v^2) - K\psi, \tag{2.15}$$

where the pressure has been non-dimensionalized by the density of fluid multiplied by the reference velocity squared, i.e. ρU_{ref}^2, and the suffix ∞ means the value at infinity. When the stream function of the boundary $\mathscr{B}$ is taken as a reference value of zero, ψ_∞ becomes

$$\psi_\infty = U_0 y + \tfrac{1}{2}Ky^2.$$

The pressure coefficient on the surface of a bluff body, which is defined by $C_{pf} = 2(p_f - p_\infty)$, p_f being the pressure on the surface, is therefore given by

$$C_{pf} = U_0^2 - u_f^2 - v_f^2, \tag{2.16}$$

where u_f and v_f denote the velocity components along the surface.

The shape of the separation streamline is represented by the set of the points (x, y) which satisfy the equation $\psi(x, y) = Q$. The asymptotic downstream spacing H between the separation streamline and the plane wall is given by the equation

$$U_0 H + \tfrac{1}{2} K H^2 = Q.$$

In the same manner as in free-streamline theories which have been developed by several authors mentioned above for the separated flow past a bluff body immersed in a uniform stream, separation of flow is also assumed to occur at the empirically given base pressure coefficient C_{pb}. The flow inside the separation streamline is ignored and the pressure coefficient over the downstream face SC is assumed constant and equal to C_{pb}. Writing the velocity components at the separation point as u_{sp} and v_{sp}, we therefore obtain from (2.15)

$$C_{pb} = U_0^2 - u_{sp}^2 - v_{sp}^2, \tag{2.17}$$

which gives a relation between the three constants U_0, K and β. A free-streamline theory presented here will not be complete without two more relations between the three constants, which would, in some way, be connected with the velocity profile in an actual boundary layer existing on the plane wall.

The general level of pressure in the front separation bubble will be determined by the separation pressure of the boundary layer. The stagnation pressure of the dividing streamline, however, will not be equal to the separation pressure, but will be greater by the amount that the total pressure on this streamline is increased by turbulent mixing with the higher velocity main flow. Although the separation pressure can be calculated with a reasonable accuracy according to the theories developed by Stratford (1959), Townsend (1960, 1962), Nishioka & Iida (1972), *et al.*, the lack of knowledge about the turbulent mixing along the dividing streamline makes it difficult to obtain theoretically the stagnation pressure on the bluff body. This situation will imply that, for the time being, the three constants mentioned above cannot be related, only by theoretical considerations, to the boundary-layer velocity profile which would be measured at the bluff body station if the bluff body were absent, and thereby some empiricism must be introduced.

We therefore assume that the maximum pressure on the wetted surface of the body occurs at the experimentally given point $z_{\max} = x_{\max} + iy_{\max}$, the maximum pressure coefficient being $C_{pf\max}$. Since, from (2.16), the maximum value of C_{pf} is U_0^2,

$$U_0 = C_{pf\max}^{\frac{1}{2}}. \tag{2.18}$$

Substitution of $z = z_{\max}$ into (2.13) also yields

$$(u - iv)_{z=z_{\max}} = 0. \tag{2.19}$$

Equations (2.18) and (2.19) are the two relations required.

Having thus established the theory, we now proceed to work out a few examples and to compare theoretical results with experimental measurements.

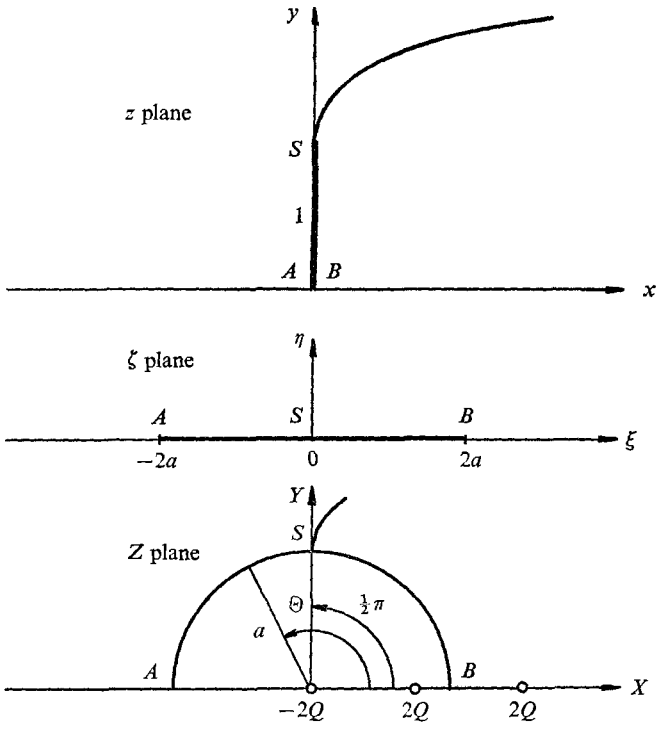

FIGURE 2. Physical plane and transform planes for normal plate.

3. Normal plate

Let the complex planes z, ζ and Z be mutually related by the equations

$$z = Z - (a^2/Z), \tag{3.1}$$

$$\zeta = Z + (a^2/Z). \tag{3.2}$$

A semicircle of radius a with its centre at the origin of the Z plane is thus transformed into a segment of a line AB on the real axis of the ζ plane which extends from $\xi = -2a$ to $\xi = 2a$ (see figure 2). The same circle in the Z plane is also mapped onto the slit ASB, which represents the normal plate of height $2a$, in the z plane (the physical plane). The height of the normal plate can be conveniently chosen as the reference length so that we may put $a = \frac{1}{2}$. Since separation occurs at the edge of the plate,

$$z_{sp} = 2ai, \quad Z_{sp} = ai, \quad \zeta_{sp} = 0,$$

where the suffix sp means the separation point.

From (3.1) and (3.2) we get

$$z \sim \zeta + O(\zeta^{-1}) \quad \text{for} \quad |\zeta| \to \infty,$$

which, when compared with (2.6), yields $k_1 = 1$ together with $k_2 = 0$ and $k_3 = 0$. The solution for W_u thus becomes

$$W_u = U_0 \zeta = U_0[Z + (a^2/Z)]. \tag{3.3}$$

By writing the equation of the semicircular projection ASB in the Z plane as $Z = ae^{i\Theta}$ $(0 \leqslant \Theta \leqslant \pi)$, we obtain from (3.1) and (3.2)

$$\zeta = 2a\cos\Theta = \xi, \quad z = 2ai\sin\Theta = iy.$$

Elimination of Θ from these equations gives

$$y^2(\xi, 0) = 4a^2 - \xi^2. \tag{3.4}$$

Therefore, upon substituting (3.4) into the expression (2.9) for W_s and performing the integration, we get

$$\begin{aligned} W_s &= \frac{K}{2\pi}\int_{-2a}^{2a} \frac{4a^2 - \xi^{*2}}{\zeta - \xi^*} d\xi^* \\ &= \frac{K}{2\pi}\left\{4a\zeta + (\zeta^2 - 4a^2)\ln\frac{\zeta - 2a}{\zeta + 2a}\right\}. \end{aligned} \tag{3.5}$$

When Q is subdivided into two parts, i.e. $Q = Q_u + Q_s$, W_Q can be written in the form

$$W_Q = W_{Qu} + W_{Qs}, \tag{3.6}$$

where $$W_{Qu} = (Q_u/\pi)F(Z), \quad W_{Qs} = (Q_s/\pi)F(Z)$$

and $$F(Z) = \ln\{(Z^2 - 2aZ\cosh\beta + a^2)/Z\}.$$

In terms of W_u, W_s, W_{Qu} and W_{Qs}, the complex velocity $\overline{w} = u - iv$ in the physical plane becomes

$$\overline{w} = Ky + \left(\frac{dW_u}{dZ} + \frac{dW_{Qu}}{dZ}\right)\Big/\frac{dz}{dZ} + \left(\frac{dW_s}{d\zeta} + \frac{dW_{Qs}}{dZ}\frac{dZ}{d\zeta}\right)\Big/\frac{dz}{d\zeta}. \tag{3.7}$$

Equations (3.1) and (3.2) yield

$$\frac{dz}{dZ} = \frac{Z^2 + a^2}{Z^2}, \quad \frac{dz}{d\zeta} = \frac{Z^2 + a^2}{Z^2 - a^2},$$

which have simple zeros at $Z = ai$ or $\zeta = 0$, i.e. the separation point. Equation (2.14) is therefore reduced to

$$\left(\frac{dW_u}{dZ} + \frac{dW_{Qu}}{dZ}\right)_{Z=ai} = 0$$

and

$$\left(\frac{dW_s}{d\zeta} + \frac{dW_{Qu}}{dZ}\frac{dZ}{d\zeta}\right)_{\zeta=0} = 0.$$

It follows from these equations that Q_u and Q_s can explicitly be obtained in the forms

$$Q_u = 2\pi a U_0 \cosh\beta, \tag{3.8}$$

$$Q_s = 8Ka^2\cosh\beta. \tag{3.9}$$

By substituting (3.8) and (3.9) into (2.12) and (3.7) and rearranging the terms, we get for the stream function

$$\begin{aligned} \psi = \tfrac{1}{2}Ky^2 + \mathscr{I}\Big\{&\left(U_0 + \frac{2Ka}{\pi}\right)\left(Z + \frac{a^2}{Z}\right) + \frac{K}{2\pi}\left(Z - \frac{a^2}{Z}\right)^2 \ln\left(\frac{Z-a}{Z+a}\right)^2 \\ &- 2a\cosh\beta\left(U_0 + \frac{4Ka}{\pi}\right)\ln\frac{Z}{Z^2 - 2aZ\cosh\beta + a^2}\Big\} \end{aligned} \tag{3.10}$$

and for the complex velocity

$$\overline{w} = Ky + \left(U_0 + \frac{4Ka}{\pi}\right)\frac{Z^2-a^2}{Z^2-2aZ\cosh\beta+a^2} + \frac{K}{\pi}\left(\frac{Z^2-a^2}{Z}\right)\ln\left(\frac{Z-a}{Z+a}\right)^2. \quad (3.11)$$

The complex velocity $\overline{w}_f$ on the front surface of the plate can conveniently be expressed in terms of the parametric variable Θ as

$$\begin{aligned}\overline{w}_f &= u_f - iv_f \\ &= i\left(U_0 + \frac{4Ka}{\pi}\right)\frac{\sin\Theta}{\cos\Theta-\cosh\beta} + i\frac{2Ka}{\pi}\sin\Theta\ln(\tan^2\tfrac{1}{2}\Theta),\end{aligned} \quad (3.12)$$

where Θ is in the range $\frac{1}{2}\pi \leqslant \Theta \leqslant \pi$. Hence, the pressure coefficient on the front surface of the plate becomes

$$C_{pf} = U_0^2 - v_f^2. \quad (3.13)$$

The velocity v_{sp} at the separation point on the edge of the plate is obtained by putting $\Theta = \frac{1}{2}\pi$ in (3.12):

$$v_{sp} = \left(U_0 + \frac{4Ka}{\pi}\right)\Big/\cosh\beta. \quad (3.14)$$

Therefore, (2.17) and (3.14) yield

$$\cosh\beta = [U_0 + (4Ka/\pi)]/(U_0^2 - C_{pb})^{\frac{1}{2}}. \quad (3.15)$$

If the right-hand side of (3.15) is greater than unity, β is real, while if it happens to be less than unity, β must be an imaginary quantity of the form $i\delta$, where δ is real, since $\cosh i\delta = \cos\delta$.

We now proceed to estimate values of U_0, K and β on the basis of experimental data which are available at present. According to experiments by Good & Joubert (1968), pressures on the upstream face of the normal plate located in the smooth-wall boundary layer are determined by a wall similarity law of the form

$$C_{pf} = \left(\frac{u_\tau}{U_{\text{ref}}}\right)^2\left\{g_1(y)\log_{10}\frac{hu_\tau}{\nu} + g_2(y)\right\}. \quad (3.16)$$

Here h is the height of the plate, u_τ is the frictional velocity, ν is the kinematic viscosity and g_1 and g_2, which are given in Good & Joubert's paper in a figure, are functions of y. For values of y less than 0·8, the pressure follows this wall law up to $h/\delta = 1{\cdot}75$, where δ is the thickness of the boundary layer. Equation (3.16) gives a maximum pressure coefficient at about $y = 0{\cdot}6$. With the free-stream velocity outside the boundary layer chosen as U_{ref}, equation (3.16) gives the pressure distribution on the front surface of the plate in terms of the height of the plate and the characteristics of the boundary layer in which the plate is immersed. Denoting the location of a maximum pressure by $y = y_{\max}$, we have from (2.18) and (3.16)

$$U_0 = \frac{u_\tau}{U_{\text{ref}}}\left\{g_1(y_{\max})\log_{10}\frac{hu_\tau}{\nu} + g_2(y_{\max})\right\}^{\frac{1}{2}} \quad (3.17)$$

and also from (2.19)

$$\left(U_0 + \frac{4Ka}{\pi}\right)\frac{\sin\Theta_m}{\cos\Theta_m-\cosh\beta} + \frac{2Ka}{\pi}\sin\Theta_m\ln(\tan^2\tfrac{1}{2}\Theta_m) = 0, \quad (3.18)$$

where

$$\Theta_m = \sin^{-1}(y_{\max}/2a).$$

Moreover, Good & Joubert (1968) have shown that the base-pressure coefficient C_{pb} is given by

$$C_{pb} = -\left(\frac{u_\tau}{U_{\text{ref}}}\right)^2 \left\{152 \log_{10} \frac{hu_\tau}{\nu} - 147 + P\phi(h/\delta)\right\}. \tag{3.19}$$

Here P is constant for turbulent boundary layers with zero pressure gradient and ϕ is a universal function of h/δ, which is tabulated in their paper. The value of C_{pb} in (3.15) can therefore be computed from (3.19). When h/δ is less than 0·5, $P\phi(h/\delta)$ is negligibly small and thus C_{pb} obeys a wall similarity law in the sense that $C_{pb}(U_{\text{ref}}/u_\tau)^2$ can be described as a function of hu_τ/ν only.

Eliminating β from (3.15) and (3.18), we obtain K explicitly in terms of U_0, C_{pb} and Θ_m as follows:

$$K = \frac{\pi}{8a}\{b + (b^2 + 4c)^{\frac{1}{2}}\},$$

where

$$b = (U_0^2 - C_{pb})^{\frac{1}{2}}\{\cos\Theta_m - (\ln\tan\tfrac{1}{2}\Theta_m)^{-1}\} - U_0,$$
$$c = U_0(U_0^2 - C_{pb})^{\frac{1}{2}}/\ln\tan\tfrac{1}{2}\Theta_m.$$

Figure 3 compares the theoretical pressure distributions on the front surface of the normal plate with the experimental results of Good & Joubert (1968). Two theoretical curves which correspond to $y_{\max} = 0{\cdot}60$ and 0·65, respectively, have been included. The present theory shows good agreement with measurements except in the region of small y, where the theory predicts larger pressures than the measurements. This discrepancy is almost indistinguishable for small h/δ, but it becomes sensible as h/δ increases. It should also be noted that, as h/δ becomes larger, the theoretical curve for $y_{\max} = 0{\cdot}65$ gives better agreement with experimental measurements than that for $y_{\max} = 0{\cdot}60$, and vice versa.

The drag coefficient C_D, which is defined as the drag divided by $\frac{1}{2}\rho(U_{\text{ref}})^2 h$, is given by

$$C_D = 2\int_0^1 (p_f - p_b)\,dy = \int_0^1 (C_{pf} - C_{pb})\,dy. \tag{3.20}$$

Theoretical values of C_D computed by substituting (3.13) and (3.19) into (3.20) are compared in table 1 with experimental values which have been obtained from an empirical formula

$$C_D = \left(\frac{u_\tau}{U_{\text{ref}}}\right)^2 \left\{277 \log_{10} \frac{hu_\tau}{\nu} - 268 + P\phi(h/\delta)\right\}$$

(Good & Joubert 1968). Table 1 shows that they agree to within 2 per cent.

For bluff bodies in an unbounded uniform stream, Roshko (1955) has demonstrated that the ratio of the velocity at the separation point to the free-stream velocity, which will be denoted by k, is almost the same for different bluff bodies under similar wake conditions, and a suitable mean value of k is 1·4. In this connexion it is interesting to note that the ratio v_{sp}/U_0 takes a constant value of 1·44 when h/δ is less than about 0·5, as is shown in the last column of table 1. Since

$$C_{pb}/U_0^2 = 1 - (v_{sp}/U_0)^2, \tag{3.21}$$

this fact suggests that the value of U_0 can directly be estimated from experimental data of C_{pb} in the region of wall similarity law.

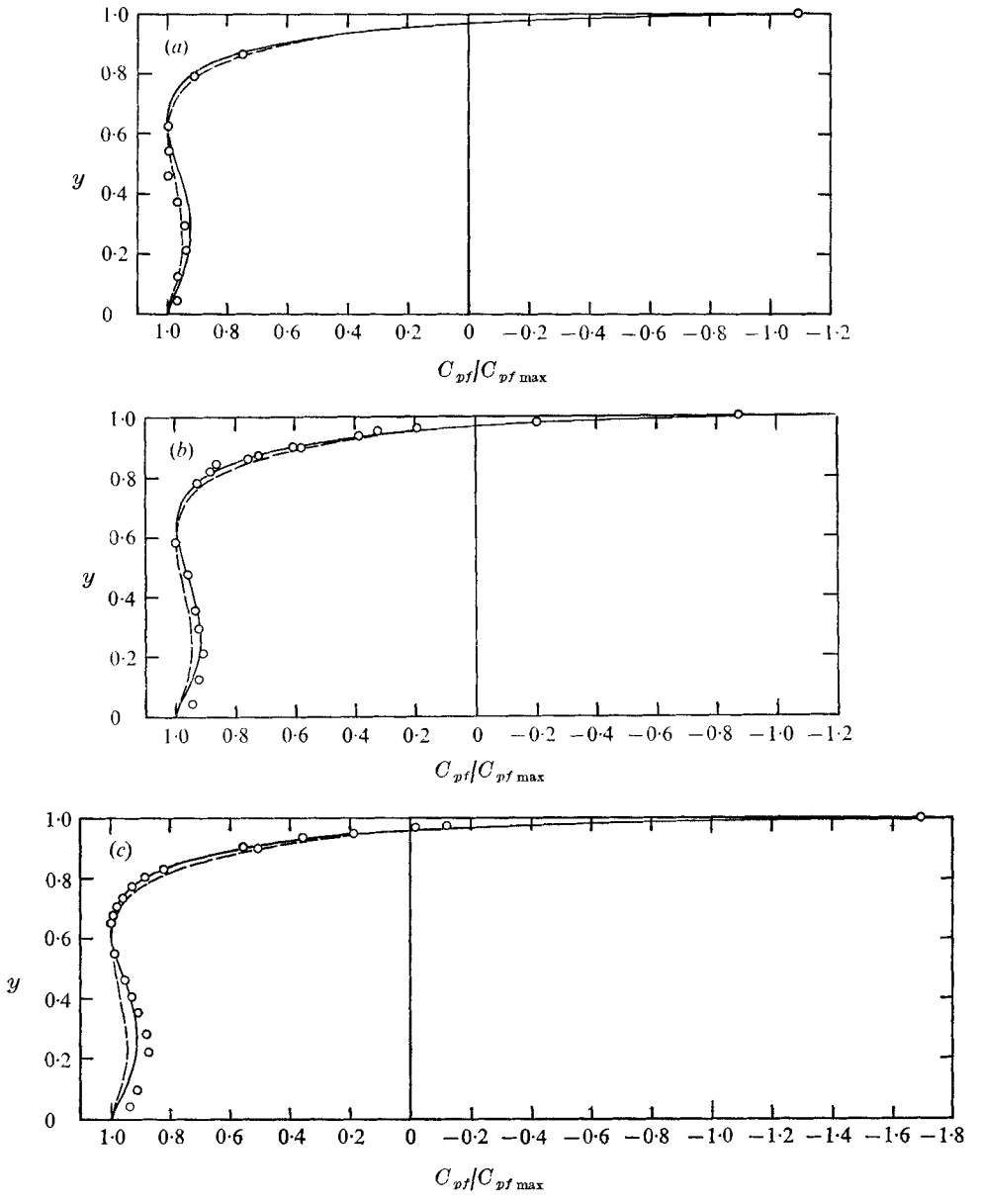

FIGURE 3. Pressure distributions on the front surface of normal plate. ○, experimental points of Good & Joubert (1968); – –, present theory, $y_{\max} = 0{\cdot}60$; ——, present theory, $y_{\max} = 0{\cdot}65$.

	u_τ/U_{ref}	hu_τ/ν	h/δ	U_0	K	$\cosh\beta$	U_0	K	$\cosh\beta$
				($y_{\max} = 0{\cdot}60$)			($y_{\max} = 0{\cdot}65$)		
(*a*)	0·0375	268	0·144	0·536	0·674	1·247	0·536	0·778	1·331
(*b*)	0·0375	2150	1·15	0·683	0·901	1·194	0·683	1·041	1·279
(*c*)	0·0348	8210	1·75	0·707	0·977	1·145	0·707	1·132	1·230

h/δ	u_τ/U_{ref}	hu_τ/ν	C_D Experiment	C_D Theory	v_{sp}/U_0
0·082	0·0348	385	0·54	0·54	1·44
0·103	0·0360	291	0·54	0·53	1·44
0·144	0·0375	268	0·57	0·56	1·44
0·219	0·0348	1030	0·69	0·68	1·44
0·309	0·0360	873	0·71	0·70	1·44
0·383	0·0375	716	0·74	0·73	1·44
0·658	0·0348	3080	0·87	0·86	1·46
0·823	0·0360	2330	0·91	0·90	1·48
1·15	0·0375	2150	1·06	1·04	1·54
1·75	0·0348	8210	1·29	1·27	1·64
2·34	0·0358	6301	1·60	1·56	1·81

TABLE 1. Drag coefficient C_D and the ratio v_{sp}/U_0. Since theoretical values of C_D and v_{sp}/U_0 for $y_{\max} = 0{\cdot}60$ and $0{\cdot}65$ are almost the same, only those for $y_{\max} = 0{\cdot}60$ are shown in this table.

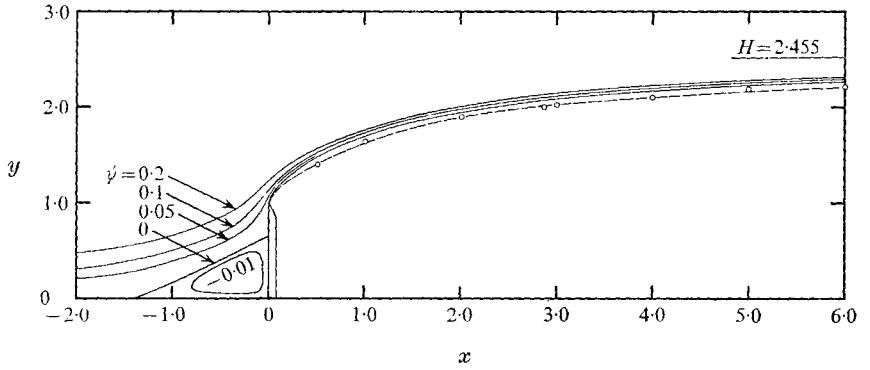

FIGURE 4. Streamlines around normal plate. ——, present theory, $U_0 = 0{\cdot}713$, $K = 1{\cdot}227$, $\cosh\beta = 1{\cdot}161$; O−−O, experimental separation streamline (Good & Joubert 1968), $h/\delta = 2{\cdot}34$, $hu_\tau/\nu = 6301$, $u_\tau/U_{\text{ref}} = 0{\cdot}0358$.

In figure 4 a few theoretical streamlines around the normal plate are shown, together with the separation streamline measured by Good & Joubert (1968). The shape of the front separation bubble is very similar to that observed experimentally by flow visualization techniques. It is also noteworthy that the theoretical separation streamline is very close to the experimental one in the range $0 \leqslant x \leqslant 6{\cdot}0$. Further downstream the experimental streamline approaches the plane wall until it reattaches to the plane wall, whereas the theoretical one approaches an asymptotic ordinate $H = 2{\cdot}455$.

4. Semicircular projection

Consider the transformations

$$z = Z - a^2 - \frac{a^2(1-a^2)}{Z-a^2}, \tag{4.1}$$

$$\zeta = Z + \frac{a^2}{Z}, \tag{4.2}$$

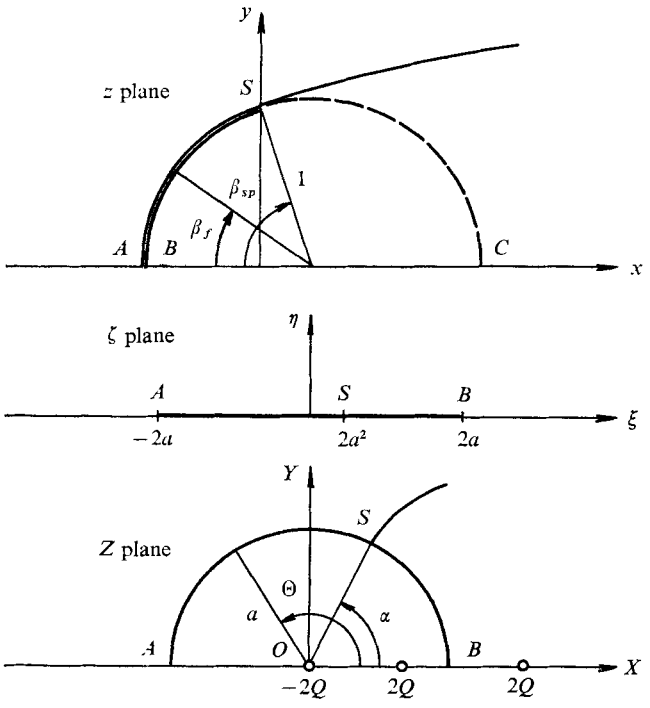

FIGURE 5. Physical plane and transform planes for semicircular projection.

where a is a real constant defined by

$$a = \cos\alpha, \tag{4.3}$$

α being real. As shown in figure 5, the circular arc slit ASB, of which the section AS represents the wetted surface of the semicircular projection ASC in the z plane, is thereby mapped onto a segment of a line AB which lies on the real axis of the ζ plane in the range $|\xi| \leqslant 2a$, and also onto a semicircle of radius a in the Z plane. The radius of the semicircle in the z plane is unity and its centre is at $(\Delta, 0)$, where $\Delta = 1 - 2a^2 = -\cos 2\alpha$. This implies that the radius of the semicircle has been chosen as the representative length. Moreover, the separation point S in the physical plane, which is

$$z_{sp} = 2ai\sin\alpha,$$

is mapped onto

$$\zeta_{sp} = 2a^2, \quad Z_{sp} = ae^{i\alpha} \tag{4.4a, b}$$

in the ζ and Z planes respectively. From (4.4b) it follows that α represents the angle between OS and OB in the Z plane. The angle α is related to the separation angle β_{sp} in the z plane by

$$\beta_{sp} = \pi - 2\alpha.$$

The semicircle in the Z plane can conveniently be expressed in the form $Z = ae^{i\Theta}$ $(0 \leqslant \Theta \leqslant \pi)$. The segment of the line AB in the ζ plane thereby becomes

$\xi = 2a\cos\Theta$, and the ordinate of the circular arc slit ASB in the z plane is written as

$$y = \frac{2a\sin\Theta(1-a\cos\Theta)}{1-2a\cos\Theta+a^2}. \tag{4.5}$$

Equation (4.5) and the relation $\cos\Theta = \xi/2a$ lead to

$$y^2(\xi,0) = \frac{1}{4}\frac{(\xi-2)^2(4a^2-\xi^2)}{(\xi-a^2-1)^2}. \tag{4.6}$$

Substituting (4.6) into (2.9) and performing the integration, we obtain

$$\begin{aligned} W_s &= \frac{K}{2\pi}\int_{-2a}^{2a}\frac{y^2(\xi^*,0)}{\zeta-\xi^*}\,d\xi^* \\ &= \frac{K}{8\pi}\left\{4aJ_1 - J_2\ln\frac{\zeta-2a}{\zeta+2a} + J_3\ln\left(\frac{a-1}{a+1}\right)^2 + \frac{4aJ_4}{(a^2-1)^2}\right\}, \end{aligned} \tag{4.7}$$

where

$$J_1 = \zeta+2(a^2-1), \quad J_2 = (\zeta-2)^2(4a^2-\zeta^2)/(\zeta-a^2-1)^2,$$

$$J_3 = -(a^2-1)^2\left\{\frac{4a^2}{\zeta-a^2-1} + \left(\frac{a^2-1}{\zeta-a^2-1}\right)^2\right\},$$

$$J_4 = -(a^2-1)^4/(\zeta-a^2-1).$$

Since $z \sim \zeta + O(\zeta^{-1})$ for $|\zeta| \to \infty$, the expressions for W_u and W_Q are the same as (3.3) and (3.6), respectively. In view of (4.4), equation (2.14) can be written as

$$\left(\frac{dW_u}{dZ} + \frac{dW_{Qu}}{dZ}\right)_{Z=ae^{i\alpha}} = 0,$$

$$\left(\frac{dW_s}{d\zeta} + \frac{dW_{Qs}}{dZ}\frac{dZ}{d\zeta}\right)_{\zeta=2a^2} = 0,$$

which yield

$$Q_u = -2\pi a U_0(a-\cosh\beta), \tag{4.8}$$

$$Q_s = -Ka(a-\cosh\beta)\left\{6a + (3a^2-1)\ln\left(\frac{1-a}{1+a}\right)\right\}. \tag{4.9}$$

Substituting (3.3), (4.7) and (3.6), with Q_u and Q_s given by (4.8) and (4.9), into (3.7), we obtain after straightforward but lengthy calculations

$$\begin{aligned} \overline{w} &= u - iv \\ &= Ky + U_0\frac{(Z^2-a^2)(Z-a^2)^2}{Z^2(Z^2-2aZ\cosh\beta+a^2)} \\ &\quad + \frac{K}{\pi}\frac{Z^2-a^2}{Z^2(Z-1)^2}\left\{\frac{a(L_1+2aL_2\cosh\beta)}{Z^2-2aZ\cosh\beta+a^2} + \frac{1}{4}\frac{L_3(Z^2-2Z+a^2)}{Z(Z-1)(Z-a^2)}\ln\left(\frac{Z-a}{Z+a}\right)^2\right. \\ &\quad \left. + \frac{1}{2}\frac{Z(L_4+2aL_5\cosh\beta)}{(Z-1)(Z-a^2)(Z^2-2aZ\cosh\beta+a^2)}\ln\left(\frac{1-a}{1+a}\right)\right\}. \end{aligned} \tag{4.10}$$

Here the L_i are defined by

$$L_1 = (Z^2+a^2)^2+3(a^2+1)^2Z^2-(5a^2+3)Z(Z^2+a^2),$$

$$L_2 = 2Z(Z^2+a^2)-(a^2+3)Z^2, \quad L_3 = Z^2(Z-1)^2+(Z^2-a^2)^2,$$

$$L_4 = -2a^2(3a^2-1)(Z^4+a^4)+4a^2(2a^4+3a^2-1)Z(Z^2+a^2) - (3a^8+20a^6+2a^4-1)Z^2,$$

$$L_5 = (3a^2-1)(Z^4+a^4)-(3a^2-1)(a^2+3)Z(Z^2+a^2)+(a^2+1)(a^4+8a^2-3)Z^2.$$

The complex velocity on the wetted surface AS, which will be denoted by $\bar{w}_f$, is obtained by substituting $Z = ae^{i\Theta}$ ($\alpha \leqslant \Theta \leqslant \pi$) into (4.10). The result is

$$\begin{aligned}\bar{w}_f &= u_f - iv_f \\ &= 2Ka\frac{\sin\Theta(1-a\cos\Theta)}{1-2a\cos\Theta+a^2}+U_0(M_1+iM_2)N \\ &\quad+\frac{K}{\pi}\left\{\left(\frac{M_1+iM_2}{M_3}\right)a(L_1^*+2aL_2^*\cosh\beta)N\right. \\ &\quad+\left(\frac{M_4+iM_5}{M_3^4}\right)(\ln\tan^2\tfrac{1}{2}\Theta+i\pi)\,2aL_3^*\sin\Theta(a\cos\Theta-1) \\ &\quad\left.+\frac{1}{2}\left(\frac{M_4+iM_5}{M_3^4}\right)(L_4^*+2aL_5^*\cosh\beta)N\ln\left(\frac{1-a}{1+a}\right)\right\}, \qquad (4.11)\end{aligned}$$

where

$$M_1 = a^2\sin 2\Theta-2a\sin\Theta, \quad M_2 = a^2\cos 2\Theta-2a\cos\Theta+1, \quad M_3 = 1-2a\cos\Theta+a^2,$$

$$M_4 = a^3\sin 3\Theta-a^2(a^2+3)\sin 2\Theta+a(3a^2+2)\sin\Theta,$$

$$M_5 = a^3\cos 3\Theta-a^2(a^2+3)\cos 2\Theta+a(3a^2+4)\cos\Theta-(3a^2+1),$$

$$N = \sin\Theta/(\cos\Theta-\cosh\beta), \quad L_1^* = 4a^2\cos^2\Theta-2a(5a^2+3)\cos\Theta+3(a^2+1)^2,$$

$$L_2^* = 4a\cos\Theta-(a^3+3), \quad L_3^* = M_2,$$

$$L_4^* = -4a^4(3a^2-1)\cos 2\Theta+8a^3(2a^4+3a^2-1)\cos\Theta-(3a^8+20a^6+2a^4-1),$$

$$L_5^* = 2a^2(3a^2-1)\cos 2\Theta-2a(3a^2-1)(a^2+3)\cos\Theta+(a^2+1)(a^4+8a^2-3).$$

The magnitude of velocity at the separation point S is given, after substitution of $\Theta = \alpha$ into (4.11) and some trigonometric manipulation, by

$$\begin{aligned}q_{sp} &= u_{sp}\sin\beta_{sp}+v_{sp}\cos\beta_{sp} \\ &= U_0(a^2-1)N^*+\frac{K}{\pi}\left\{3a(a^2-1)(1-2a\cosh\beta+a^2)N^*\right. \\ &\quad+2a(2a^2-1)\sin\alpha\ln\left(\frac{1-a}{1+a}\right)+4\pi a^2(1-a^2) \\ &\quad\left.-\tfrac{1}{2}[11a^4-2a^2-1-2a(7a^2-3)\cosh\beta]N^*\ln\left(\frac{1-a}{1+a}\right)\right\}, \qquad (4.12)\end{aligned}$$

where

$$N^* = \sin\alpha/(a-\cosh\beta).$$

The four undetermined constants, i.e. U_0, K, β and β_{sp}, can be determined from (2.17), (2.18) and (2.19), together with the location of the separation point which

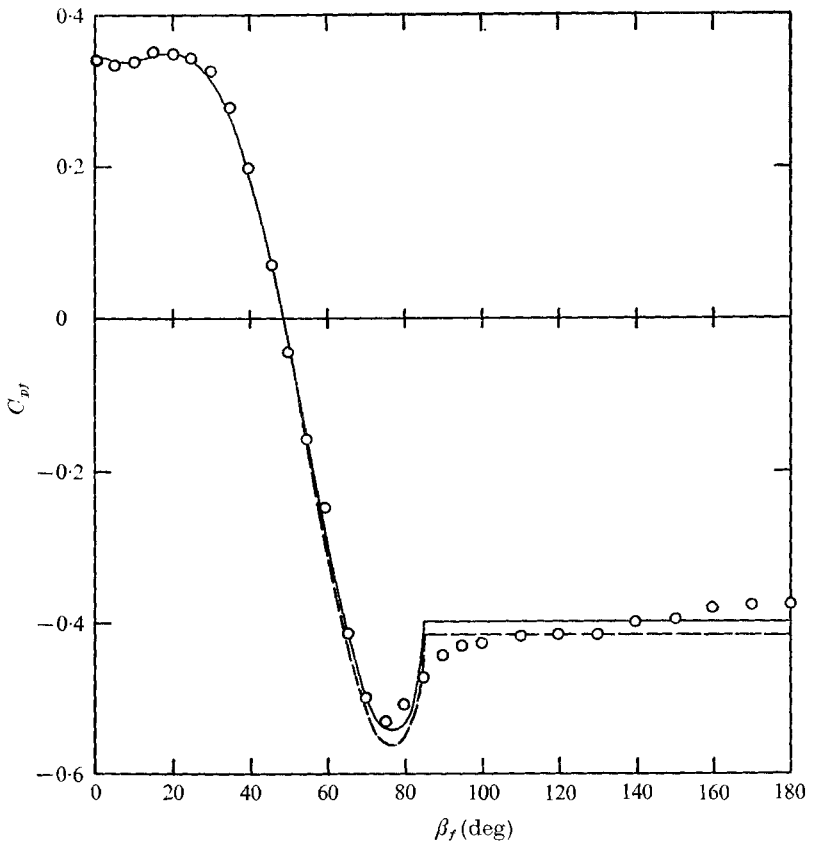

FIGURE 6. Pressure distributions on semicircular projection. ———, present theory, $\beta_{sp} = 85°$, $C_{pb} = -0{\cdot}40$; – – –, present theory, $\beta_{sp} = 85°$, $C_{pb} = -0{\cdot}42$; ○, experiment by Sakamoto & Moriya (1973), $r/\delta = 0{\cdot}268$ (r = radius of semicircular projection), $u_\tau/U_{\text{ref}} = 0{\cdot}0393$, $ru_\tau/\nu = 528$.

has been given by experiments. By eliminating β from (2.17) and (2.19), we obtain a quadratic equation for K with complicated coefficients, which can be solved anyway.

Within the authors' knowledge, experimental information about the semicircular projection attached to a plane wall is not sufficient to correlate pressure distributions on the projection and its drag coefficients with the characteristics of the turbulent boundary layer in which it is immersed. The only data available to the authors are the pressure distribution along the surface of a semicircular projection measured by Sakamoto & Moriya (1973) in the subcritical range. In figure 6 their result is compared with the theoretical surface pressure distributions for cases representing two values of C_{pb} with the same separation angle β_{sp}. Here the free-stream velocity outside the turbulent boundary layer has been chosen as the representative velocity U_{ref}. The present theory shows good general agreement with the experimental measurements except near the suction peak and in the region exposed to the separated flow, where measured pressures increase slightly towards $\beta_f = 180°$ while the theory gives

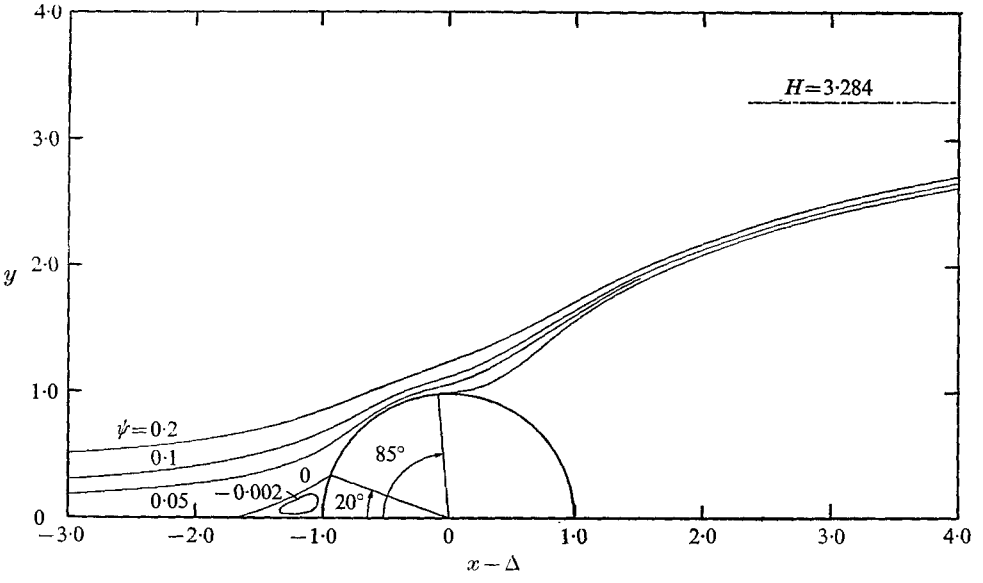

FIGURE 7. Theoretical shape of separation streamline for semicircular projection. $C_{pb} = -0{\cdot}42$, $\beta_{sp} = 85°$, $C_{f\max} = 0{\cdot}35$, $\beta_{\max} = 20°$ ($\beta_{\max}$ = angle of maximum pressure).

constant pressures. Anyway this discrepancy is so small that the surface pressure loading of the semicircular projection can be predicted accurately enough for practical use by the present theory.

Figure 7 gives the shape of the separation streamline calculated by the present theory for the case of $\beta_{sp} = 85°$, $C_{pb} = -0{\cdot}42$. In contrast to the case of the normal plate, the theoretical shape of the separation streamline seems to be reasonable within a short distance from the separation point, although detailed flow patterns around the semicircular projection have not been clarified as yet.

Finally the drag coefficients calculated by the present theory, i.e. $C_D = 0{\cdot}54$ for $C_{pb} = -0{\cdot}40$ and $C_D = 0{\cdot}56$ for $C_{pb} = -0{\cdot}42$, agreed with the measured value $C_D = 0{\cdot}55$ within 2 per cent.

5. Concluding remarks

A free-streamline theory has been developed for calculating the separated flow past a two-dimensional bluff body attached to a long plane wall on which a turbulent boundary layer exists. The velocity profile in the turbulent boundary layer which would be measured at the bluff body station if the bluff body were absent has been replaced by a hypothetical inviscid shear flow which has a constant vorticity. This model automatically yields closed streamlines in front of bluff bodies such as a normal plate and a semicircular projection, which are geometrically very similar to observed front separation bubbles. However, the lack of knowledge about turbulent mixing along the edge of the front separation bubbles introduces another empiricism into the present theory, together with the base-pressure coefficient and the separation position, which are all the empirical constants needed in the free-streamline theoryfor bluff bodies in an

unbounded uniform stream. As a result, the present theory includes three or four constants which should be determined on the basis of experimental information, the number of constants depending upon the shape of the bluff body. For bluff bodies for which these constants can be properly estimated, theoretical pressure distributions predicted by the present theory appear to be in good agreement with experimental results. Moreover, the theoretical shape of the free streamline separated from the edge of the normal plate agrees well with the measured shape for a considerable distance downstream the plate.

Although only two typical examples of bluff bodies, i.e. the normal plate and the semicircular projection, are worked out in the present paper, the method can be applied to other shapes whose wetted surface and its reflexion on the lower half of the z plane can be mapped onto a circle in the Z plane.

REFERENCES

Acrivos, A., Snowden, D. D., Grove, A. S. & Peterson, E. E. 1965 The steady separated flow past a circular cylinder at large Reynolds numbers. *J. Fluid Mech.* **21**, 737.

Arie, M., Kiya, M., Tamura, H. & Kanayama, Y. 1972 Flow about rectangular cylinders immersed in turbulent boundary layers. To be published.

Fraenkel, L. E. 1961 On corner eddies in plane inviscid shear flow. *J. Fluid Mech.* **11**, 400.

Good, M. C. & Joubert, P. N. 1968 The form drag of two-dimensional bluff-plates immersed in turbulent boundary layers. *J. Fluid Mech.* **31**, 547.

Nishioka, M. & Iida, S. 1972 Separation of turbulent boundary layer: wall pressure distribution near separation point. *Bull. J.S.M.E.* **15**, 1084.

Parkinson, G. V. & Jandali, T. 1970 A wake source model for bluff body potential flow. *J. Fluid Mech.* **40**, 577.

Roshko, A. 1955 On the wake and drag of bluff bodies. *J. Aeron. Sci.* **22**, 124.

Sakamoto, H. & Moriya, M. 1973 Study on the flow around a semicircular cylinder placed on a plane wall. *Memoirs of the Kitami Institute of Technology*, vol. 4. To be published.

Stratford, B. S. 1959 The prediction of separation of the turbulent boundary layer. *J. Fluid Mech.* **5**, 1.

Townsend, A. A. 1960 The development of turbulent boundary layers with negligible wall stress. *J. Fluid Mech.* **8**, 143.

Townsend, A. A. 1962 The behaviour of a turbulent boundary layer near separation. *J. Fluid Mech.* **12**, 536.

Woods, L. C. 1955 Two-dimensional flow of a compressible fluid past given curved obstacles with wakes. *Proc. Roy. Soc.* A **227**, 367.

Wu, T. Y. 1962 A wake model for free-streamline flow theory. *J. Fluid Mech.* **13**, 161.

Yih, C.-S. 1959 Two solutions for inviscid rotational flow with corner eddies. *J. Fluid Mech.* **5**, 36.